

# Stratospheric sulfate aerosols from ACE and SAGE III / ISS

**Adam Pastorek**<sup>1</sup>, Peter Bernath<sup>1</sup>, Chris Boone<sup>2</sup>

*1 – Department of Chemistry and Biochemistry, Old Dominion University, Virginia, USA*

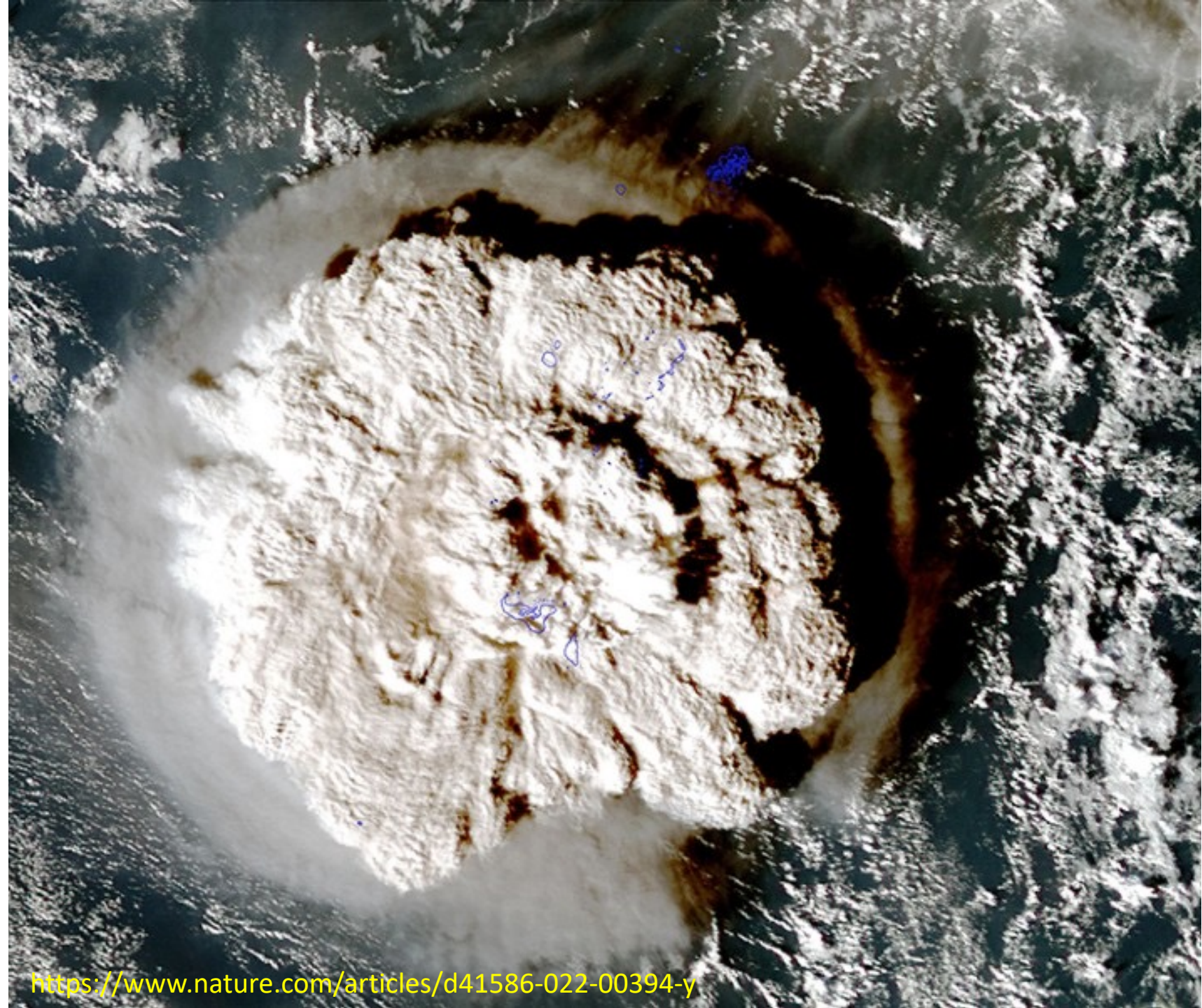
*2 – Department of Chemistry, University of Waterloo, Ontario, Canada*

# Stratospheric sulfate aerosols (SSAs)

- SSAs from volcanic eruptions play an important role in chemical and physical processes in our atmosphere
- Strong impact on climate (absorption and scattering of incoming and outgoing radiation)
- SSAs cool the surface and heat the stratosphere
- SSAs affect stratospheric chemistry (ozone depletion)
- Seed particles for polar stratospheric clouds (PSCs) → Antarctic ozone hole
- SSAs are essential components of various climate models but their contributions are **incomplete**

# Hunga Tonga-Hunga Ha'apai

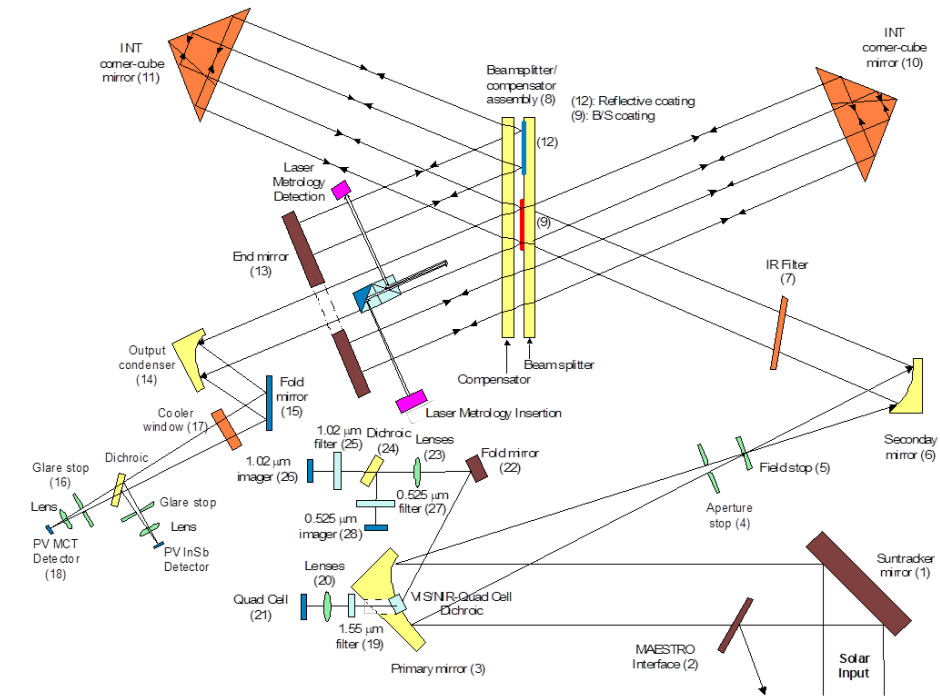
- Eruption on 15<sup>th</sup> Jan 2022
- Underwater volcano north from Tonga in South Pacific
- Comparable energy release to Tsar bomb
- Reached 57 km (mesosphere)
- Huge amounts of water injected into stratosphere
- SO<sub>2</sub> injected:  $0.41 \pm 0.02$  Tg (due to enormous water amount – OH radical)





# ACE

- The Atmospheric Chemistry Experiment (ACE) is a satellite mission onboard the Canadian satellite SCISAT
- Sun as a source for limb-geometry measurements
- Launched in 2003
- FTIR spectrometer onboard ( $0.02 \text{ cm}^{-1}$  resolution)
- 2 imagers ( $527.11 \text{ nm}$  &  $1020.55 \text{ nm}$ )
- $750 - 4400 \text{ cm}^{-1}$
- Altitude profiles of temperature, pressure, atmospheric extinction and VMRs (46 molecules)





# Processing of data

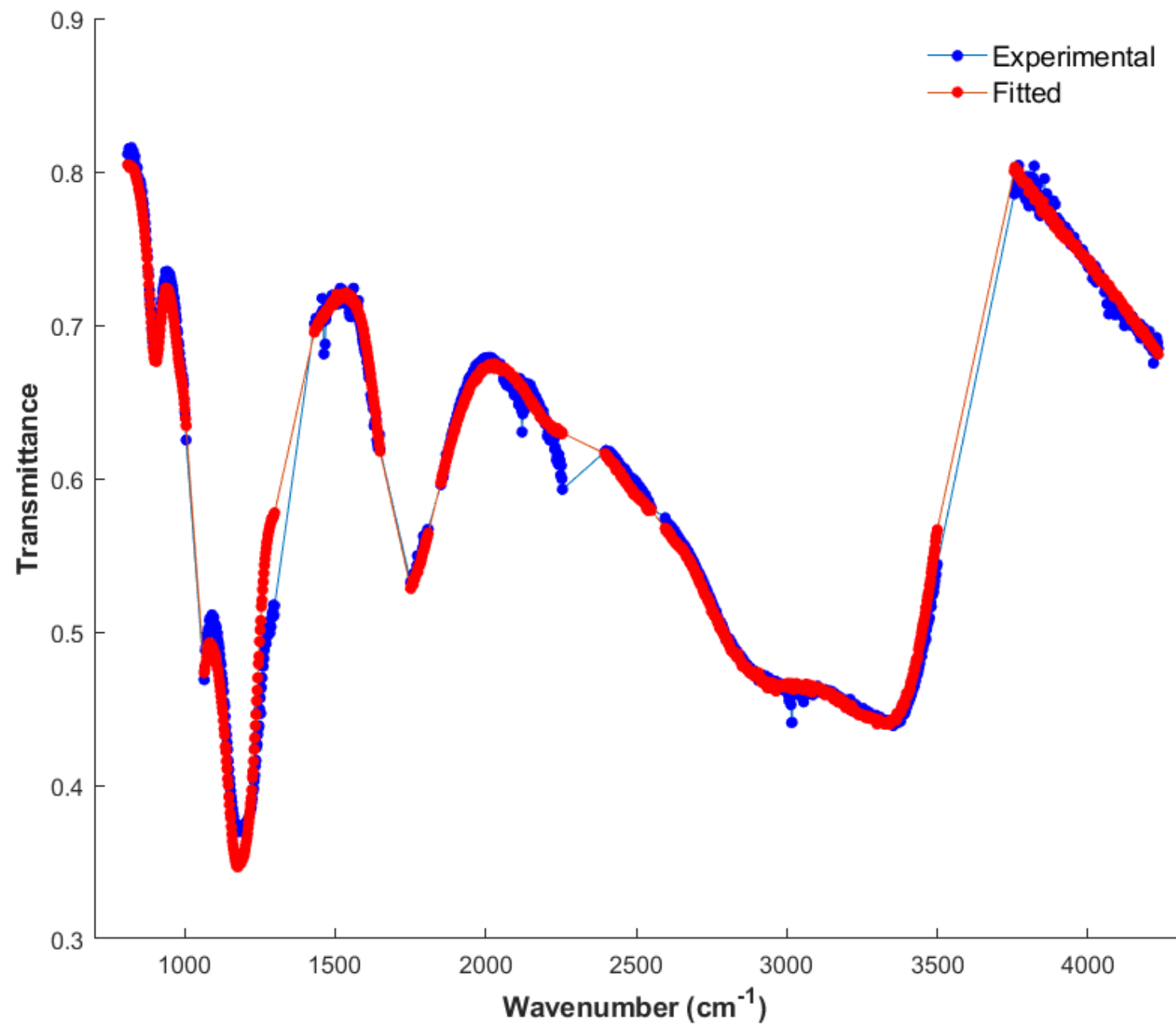
- Remove spectral features of individual molecules → transmission spectra of clouds and SSAs
- Remaining artefacts (HNO<sub>3</sub>) removed by dividing with reference spectrum
- Final residual spectrum is free from artefacts and contains background SSAs & volcanic SSAs
- Then the spectrum is fitted by variation of 4 parameters contained in the Beer-Lambert law (baseline parameter A, r<sub>m</sub>, w(H<sub>2</sub>SO<sub>4</sub>) & column density)

Baseline parameter      Extinction cross-section      Extinction coefficient

$$\tau = A \exp(-\sigma_{\text{ext}} N \ell) = A \exp(-\alpha \ell)$$

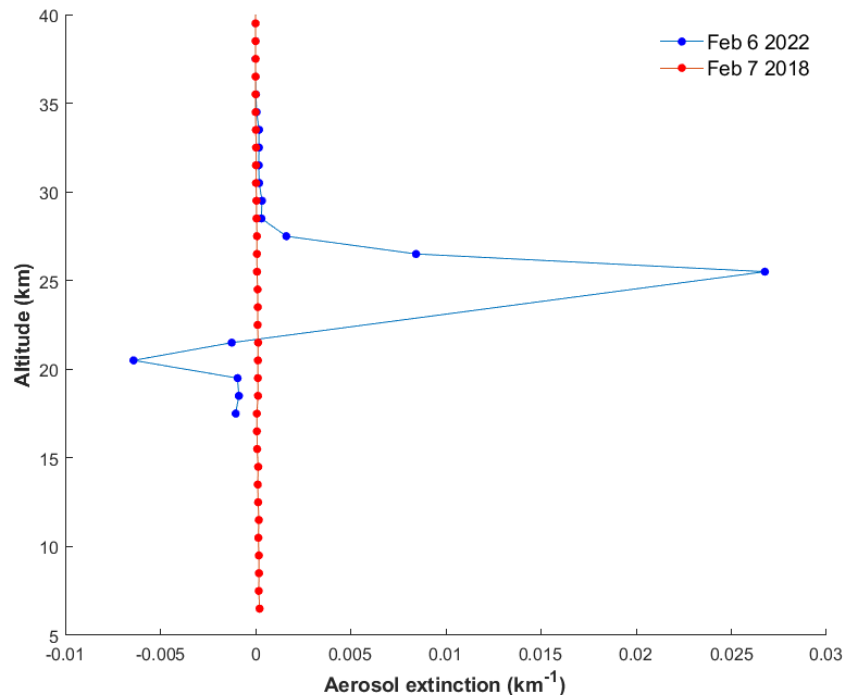
$$\sigma_{\text{ext}} = f(\nu, S, x)$$

$$n(r) = \frac{N}{\sqrt{2\pi}} \frac{1}{\ln(S)} \frac{1}{r} \exp\left[-\frac{(\ln r - \ln r_m)^2}{2 \ln^2(S)}\right]$$

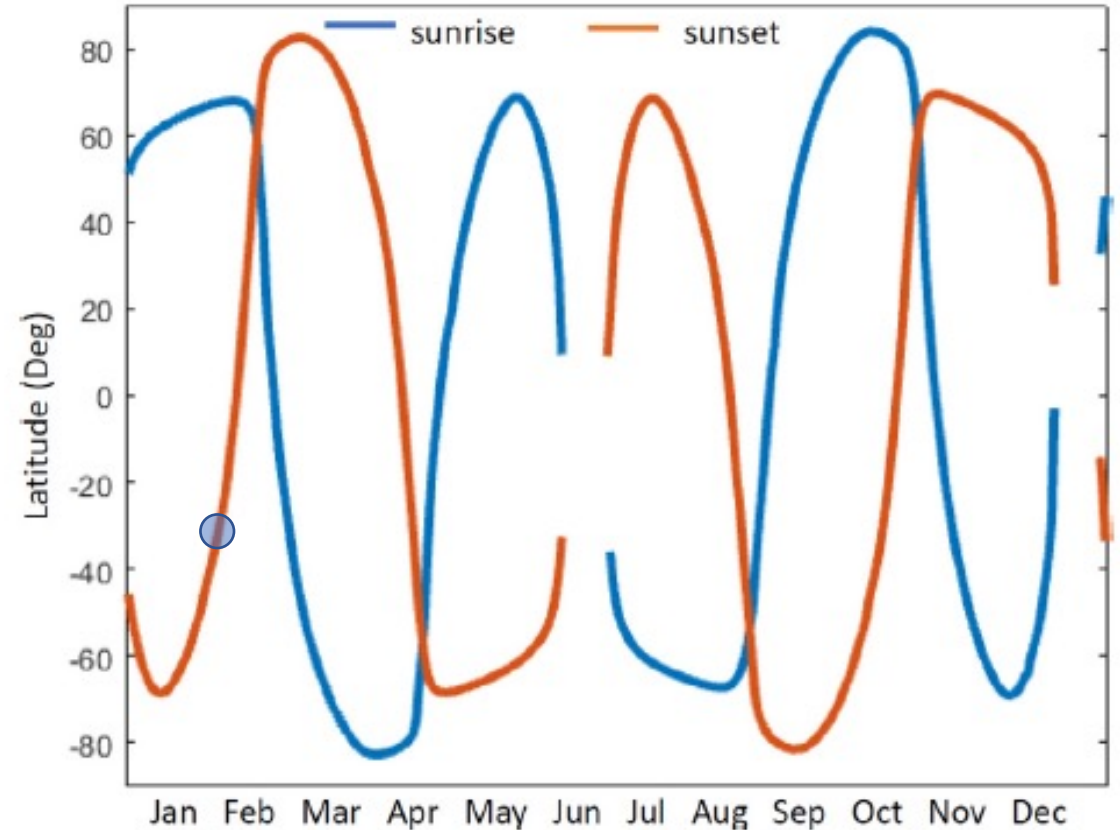


# ACE measurement & tracking of Tonga eruption

- ACE was measuring in Antarctica at the time of eruption
- Tonga plume reached by 4<sup>th</sup> Feb 2022



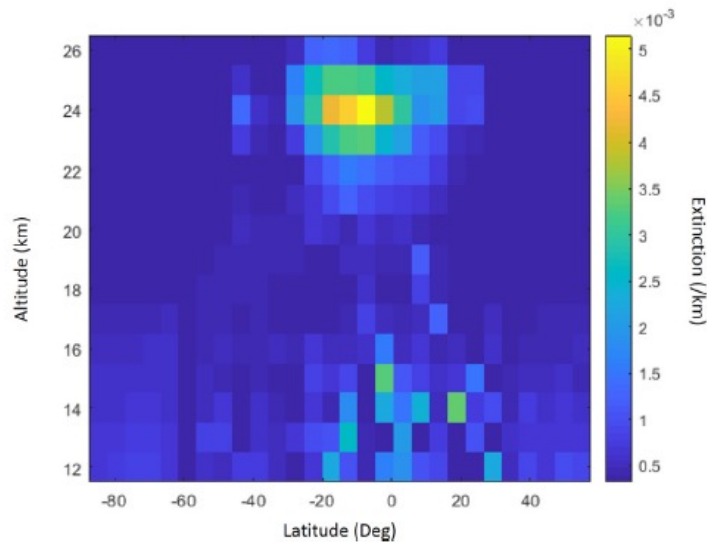
Altitude profile of aerosol extinction. Aerosol extinction at 1.02  $\mu\text{m}$  for ss99611 (ss for sunset and 99,611 is the orbit number from the start of the mission) on 6 February located at 19.85 °S and 127.59 °E. An extinction profile for a reference occultation (ss78053) recorded on 7 February 2018 without a volcanic plume is also displayed.



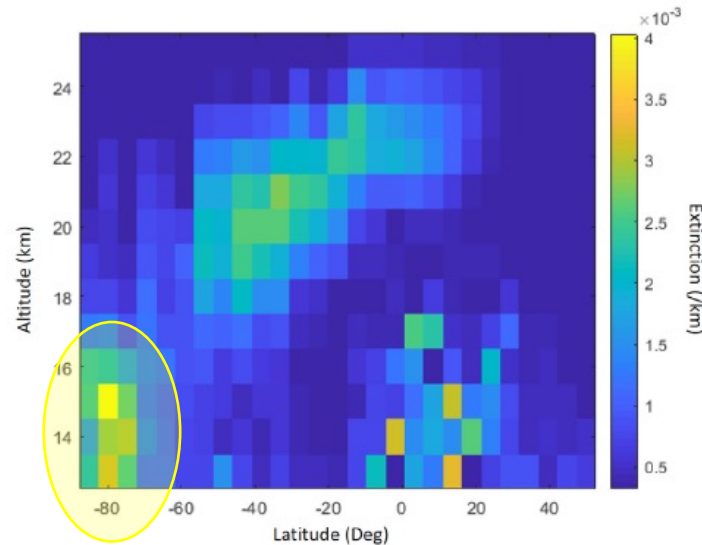
Location of ACE measurements. Latitude distribution of ACE occultations for 2021. This latitude distribution is approximately the same for each year.



# Latitude tracking of the plume



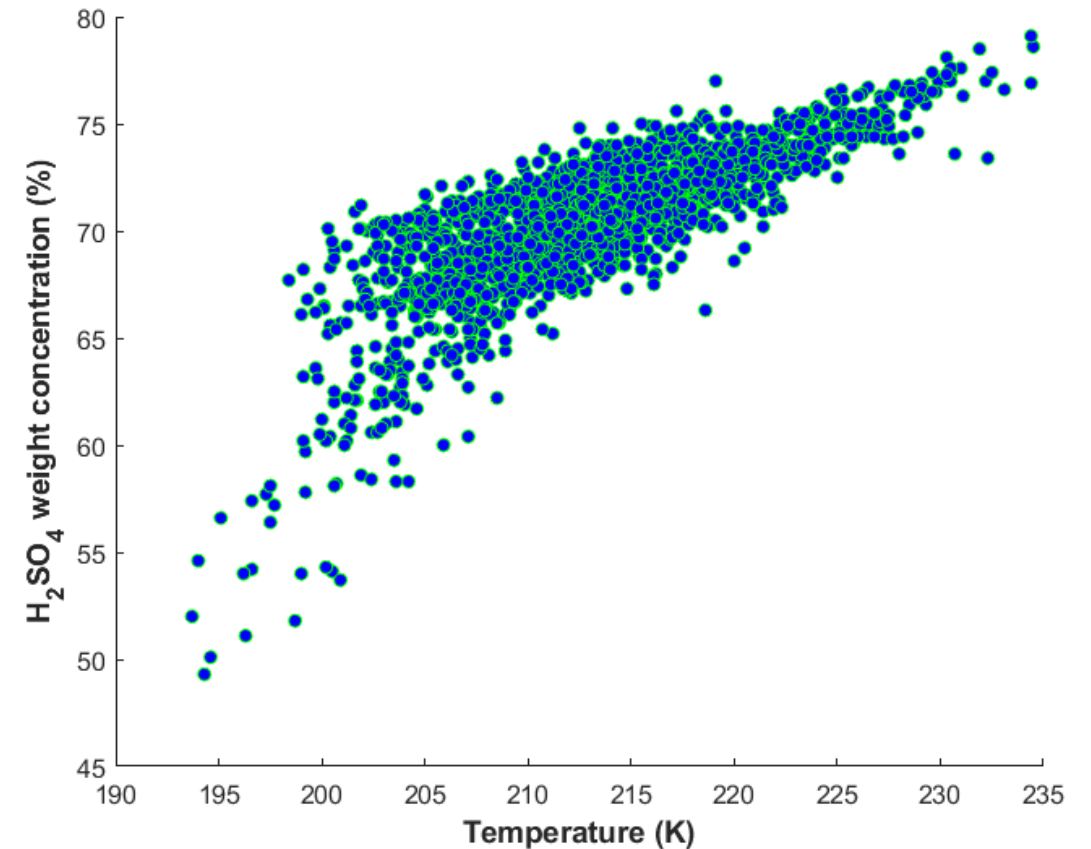
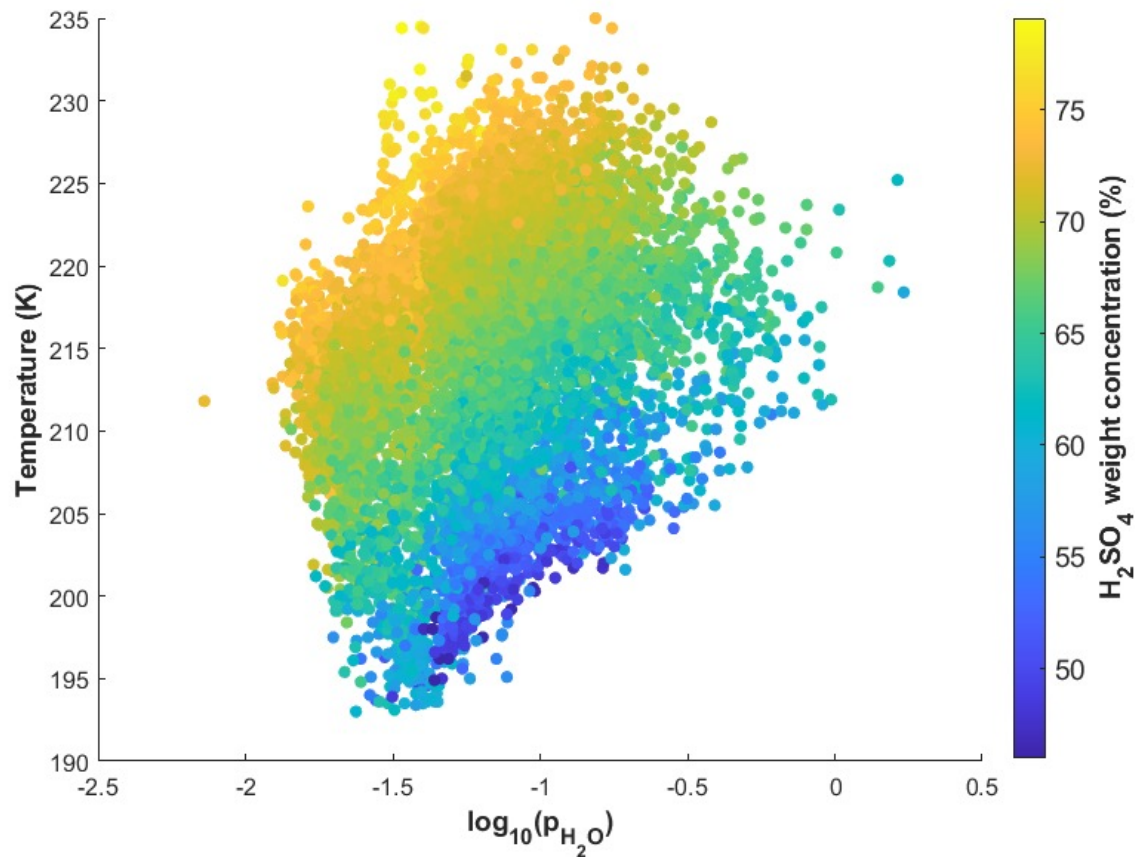
Aerosol extinction for April 2022. ACE Imager aerosol extinction at  $1.02 \mu\text{m}$  for  $5^\circ$  latitude by 1 km altitude bins.



Aerosol extinction for August 2022. ACE Imager aerosol extinction at  $1.02 \mu\text{m}$  for  $5^\circ$  latitude by 1 km altitude bins.

- During Feb 2022, the plume was between  $30^\circ\text{S}$  and  $10^\circ\text{N}$
- In Apr 2022, the plume had spread between  $40^\circ\text{S}$  and  $20^\circ\text{N}$
- In Jun 2022, the plume had reached Antarctica
- In Aug 2022, the plume had extended from  $25^\circ\text{N}$  to within polar vortex
- Still persistent in Nov 2022 and reached Arctic
- Spread all over the globe

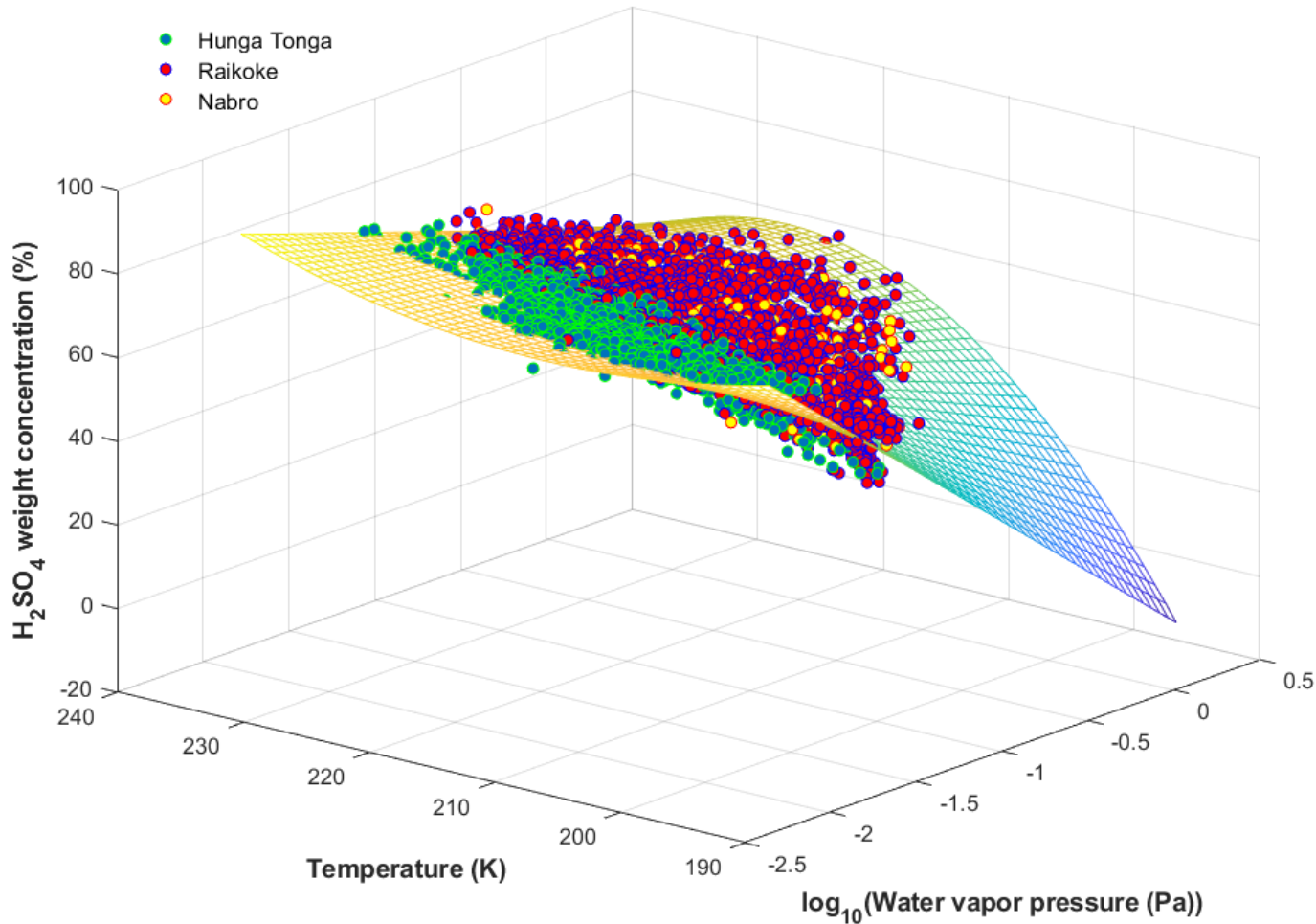
# Dependence of composition of SSAs on other variables



Composition of Tonga aerosols. H<sub>2</sub>SO<sub>4</sub> concentration (weight %) as a function temperature.

Observed composition of sulfate aerosols. The H<sub>2</sub>SO<sub>4</sub> concentration (weight %) using the color scale on the right as a function of temperature (K) and  $\log_{10}$  (H<sub>2</sub>O vapor pressure in Pa). As the temperature decreases and the water vapor pressure increases, the sulfuric acid concentration decreases. Points from Tonga, Raikoke and Nabro volcanic eruptions are included.

$R^2 = 0.88$



# Multiple linear regression

- HT + R points fitted
- N points added for visualization only
- $T$  and  $p$  dependent variables

$$w_{H_2SO_4} = -3247.97853 - 2006.27938 \cdot \log(p_{H_2O}) + 29.50612 \cdot T + 18.09112 \cdot \log(p_{H_2O}) \cdot T - 0.06570 \cdot T^2 - 0.04091 \cdot \log(p_{H_2O}) \cdot T^2$$



# Combining ACE & SAGE III measurements



750-4400  $\text{cm}^{-1}$

6500-26000  $\text{cm}^{-1}$

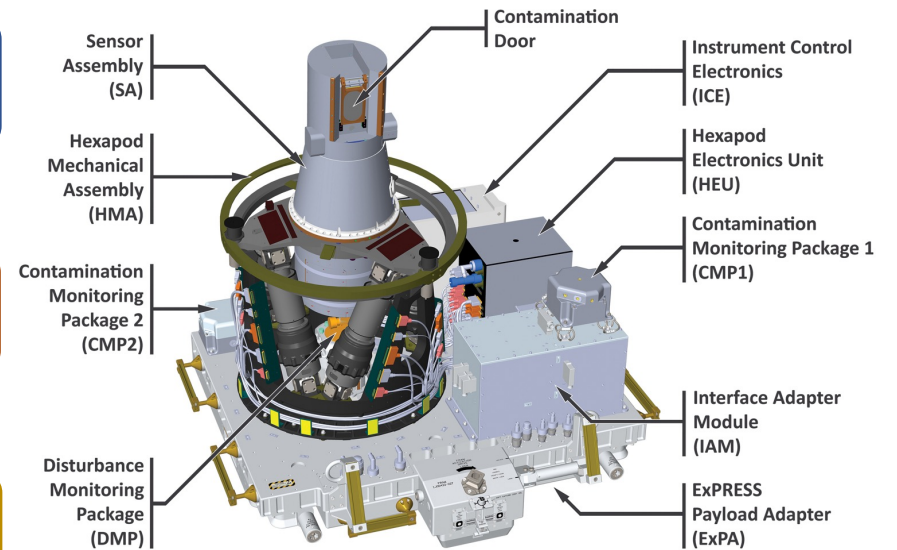
Solar occultations

Solar & lunar occultations

IR absorption  
Composition information

NIR/VIS scattering  
Particle size information

Different viewing geometry



Combining the two datasets provides more complete information on aerosol physical characteristics like  $w(\text{H}_2\text{SO}_4)$ , median radius of particles or size distribution.

# Bimodal distribution of SSAs

- Tendency of SSAs to form a bimodal distribution rather than monomodal
- For background & volcanic SSAs
- Fine & coarse mode according to particle size
- $w(\text{H}_2\text{SO}_4)$  value is shared, but  $\alpha$  are different (different  $r_m, S$ )

$$\tau = A * \exp[-\alpha L_{\text{eff}}]$$



$$\tau = A * \exp[-(\alpha_1 L_1 + \alpha_2 L_2)]$$

# Finding coincidences

- Similar air masses measured
- Overlap is better in the northern hemisphere
- Less tight in the south, but Tonga-only (long-term stability → consistent even despite larger geographical separation)

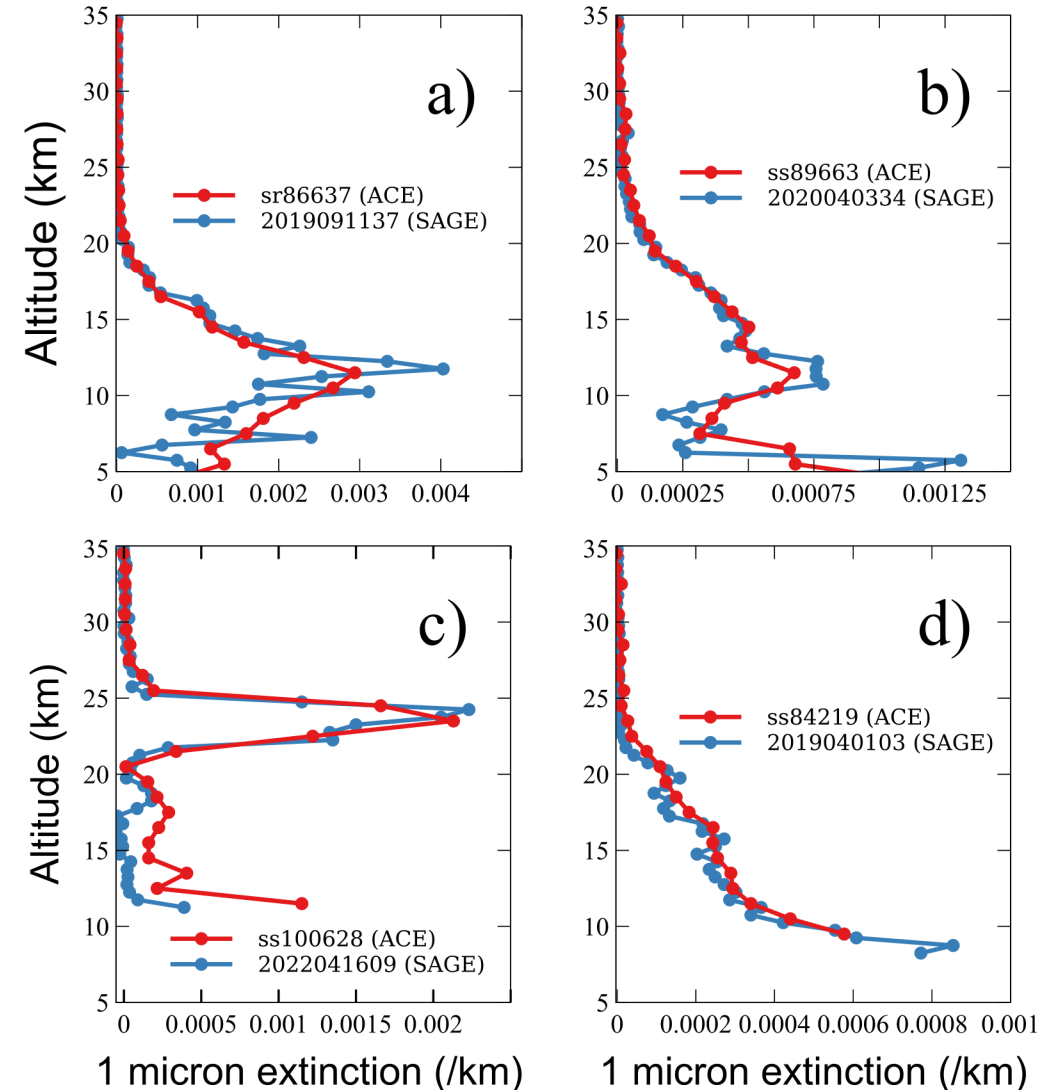
ACE event	SAGE III/ISS event	Latitude (°)	Δ time (minutes)	Δ latitude (°)	Δ longitude (°)	Type
ss84200	2019033036	58.7	1.7	0.9	0.2	Background
ss84219	2019040103	55.7	2.3	0.9	0.3	Background
sr86637	2019091137	58.0	2.0	0.2	0.4	Raikoke
sr88283	2020010112	46.9	5.5	3.0	1.5	Raikoke
ss89663	2020040334	45.5	3.3	0.7	0.7	Raikoke
sr99051	2021123021	43.7	0.7	0.1	0.3	Background
ss100628	2022041609	-28.7	1.1	0.6	0.1	Tonga
ss102428	2022081606	-26.4	17	3.4	3.2	Tonga
ss103255	2022101109	-15.0	16	4.3	3.4	Tonga



# ACE & SAGE MIR imagers

- 1  $\mu\text{m}$  imager is on board both instruments
- 1020.55 nm (ACE)
- 1021.20 nm (SAGE)
- Suitable for verification of both measurements

**Figure 1:** 1  $\mu\text{m}$  aerosol extinction for pairs of coincident ACE and SAGE III/ISS measurements. a) sr86637 [September 11, 2019, latitude 58.0  $^{\circ}\text{N}$ , longitude 157.4  $^{\circ}\text{E}$ ] and SAGE 2019091137, containing sulfates from the Raikoke eruption. b) ss89663 [April 3, 2020, latitude 45.5  $^{\circ}\text{N}$ , longitude 13.8  $^{\circ}\text{E}$ ] and SAGE 2020040334, also from the Raikoke eruption. c) ss100628 [April 16, 2022, latitude 28.7  $^{\circ}\text{S}$ , longitude 171.2  $^{\circ}\text{E}$ ] and SAGE 2022041609, containing sulfates from the Tonga eruption. d) ss84219 [April 1, 2019, latitude 55.7  $^{\circ}\text{N}$ , longitude 102.5  $^{\circ}\text{W}$ ] and SAGE 2019040103, with background-level sulfates. Note the different x-axis scales.



# Raikoke plume analysis

- Monomodal distribution unsatisfactory
- First points at lower WN are from ACE, the rest is from SAGE
- 2 solutions possible

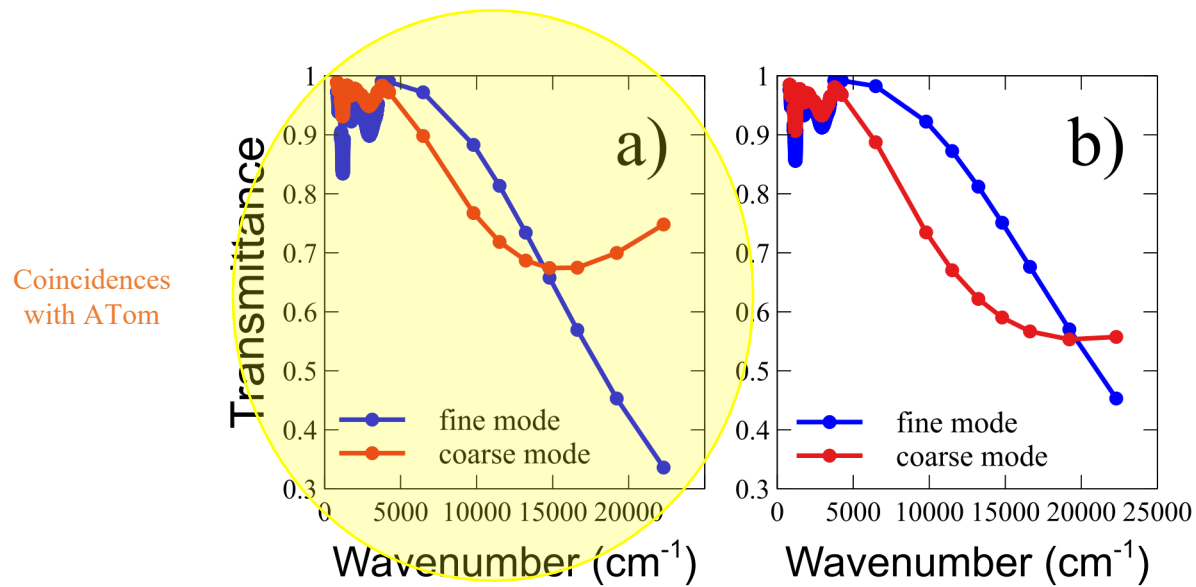


**Figure 3:** Contributions to the calculated spectrum for the fitting result in Figure 2b from the fine and coarse modes (in blue and red, respectively). The calculated spectrum is the product of the two curves. There are two solutions with nearly identical fitting quality. a)  $r_m(\text{fine}) = 0.053 \pm 0.003 \mu\text{m}$ ,  $S(\text{fine}) = 1.65$  (fixed),  $r_m(\text{coarse}) = 0.28 \pm 0.06 \mu\text{m}$ ,  $S(\text{coarse}) = 1.40 \pm 0.10$ , and  $N_o(\text{fine})/N_o(\text{coarse}) \approx 130$ . b)  $r_m(\text{fine}) = 0.059 \pm 0.003 \mu\text{m}$ ,  $S(\text{fine}) = 1.65$  (fixed),  $r_m(\text{coarse}) = 0.44 \pm 0.10 \mu\text{m}$ ,  $S(\text{coarse}) = 1.15 \pm 0.18$ , and  $N_o(\text{fine})/N_o(\text{coarse}) \approx 380$ . Reported uncertainties are random fitting errors and do not include systematic errors.

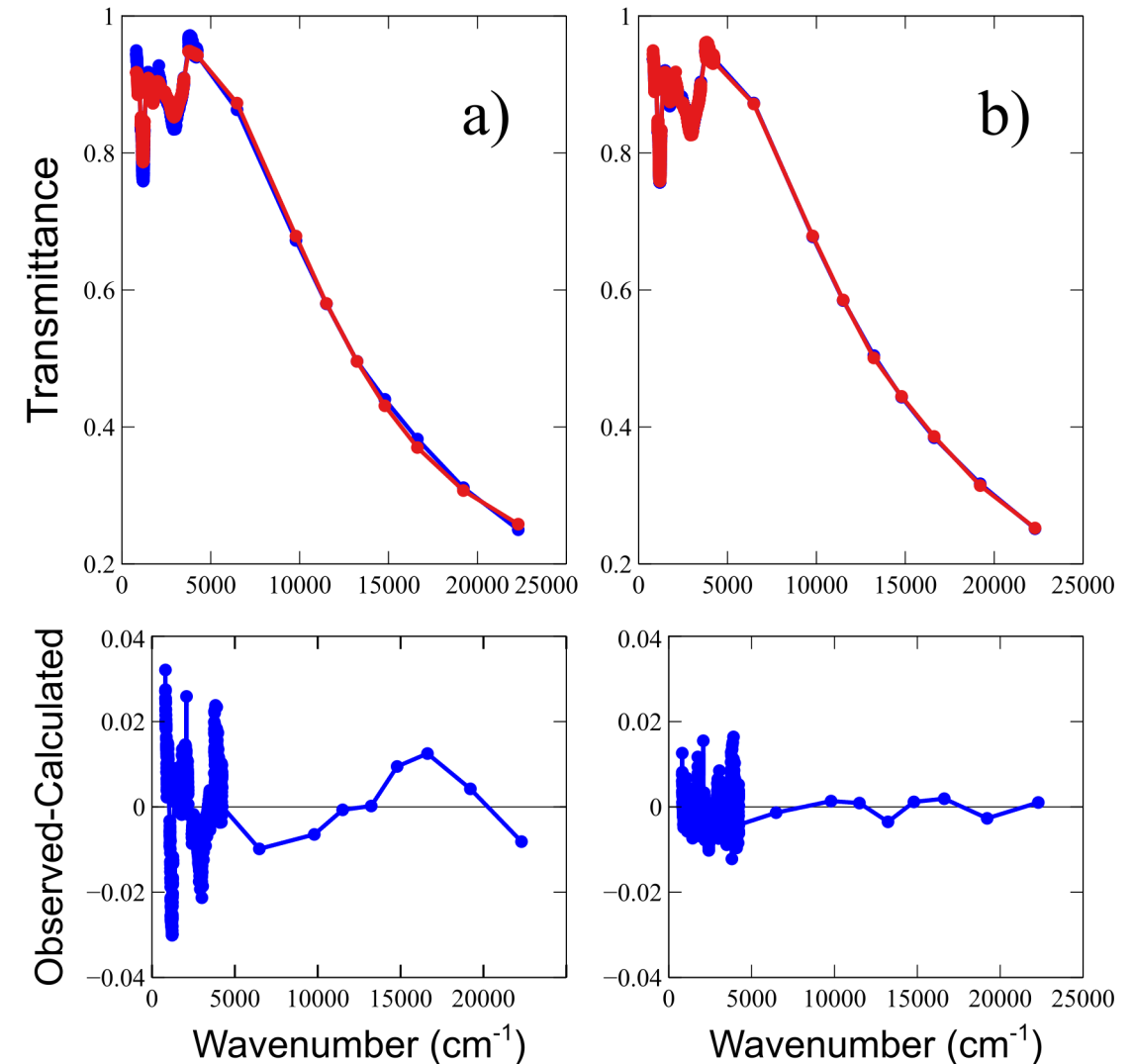


**Figure 2:** Combined ACE-FTS and SAGE III/ISS transmittance fitting results for the measurement at tangent height 15.2 km in ACE occultation sr86637. The coincident SAGE event is 2019091137. The top plots show the measurement in blue and the fitted result in red, while the bottom plot shows the residuals (observed – calculated). a) Assuming a monomodal distribution. b) Assuming a bimodal distribution.

# Tonga plume analysis

- Again, significant improvement for the bimodal distribution
- With  $S$  fixed at 1.65  $\rightarrow$  RMS  $\sim$  5-6%

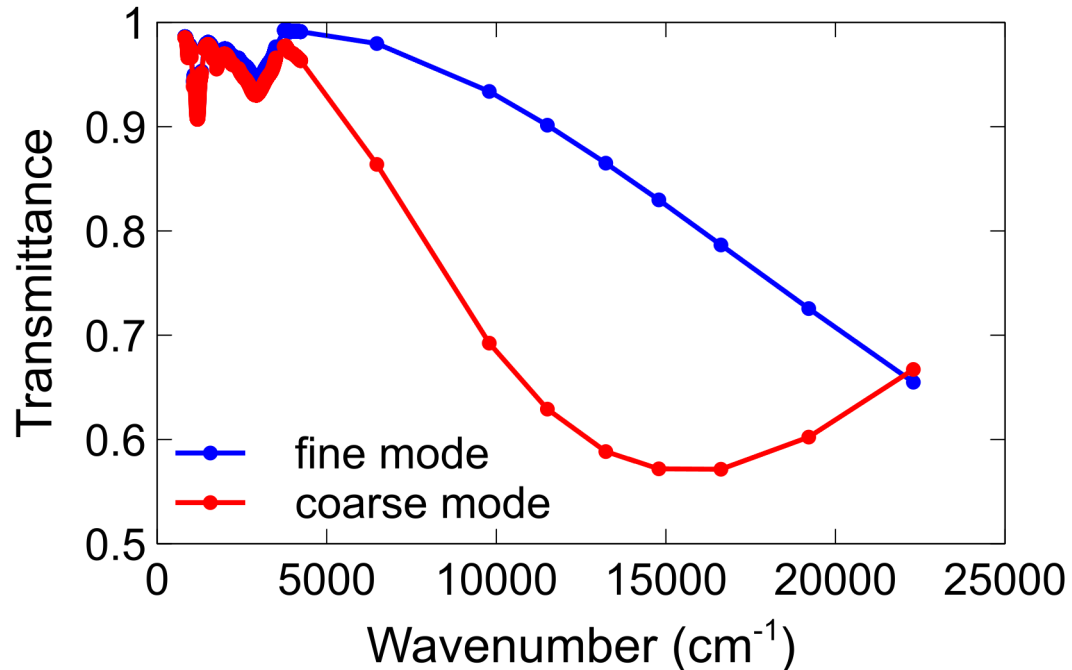


**Figure 5:** Contributions to the calculated spectrum for the fitting result in Figure 4b from the fine and coarse modes (in blue and red, respectively). The calculated spectrum is the product of the two curves.  $r_m(\text{fine}) = 0.050 \pm 0.003 \mu\text{m}$ ,  $S(\text{fine}) = 1.65$  (fixed),  $r_m(\text{coarse}) = 0.44 \pm 0.02 \mu\text{m}$ ,  $S(\text{coarse}) = 1.12 \pm 0.05$ , and  $N_o(\text{fine})/N_o(\text{coarse}) \approx 190$ . Reported uncertainties are random fitting errors and do not include systematic errors.

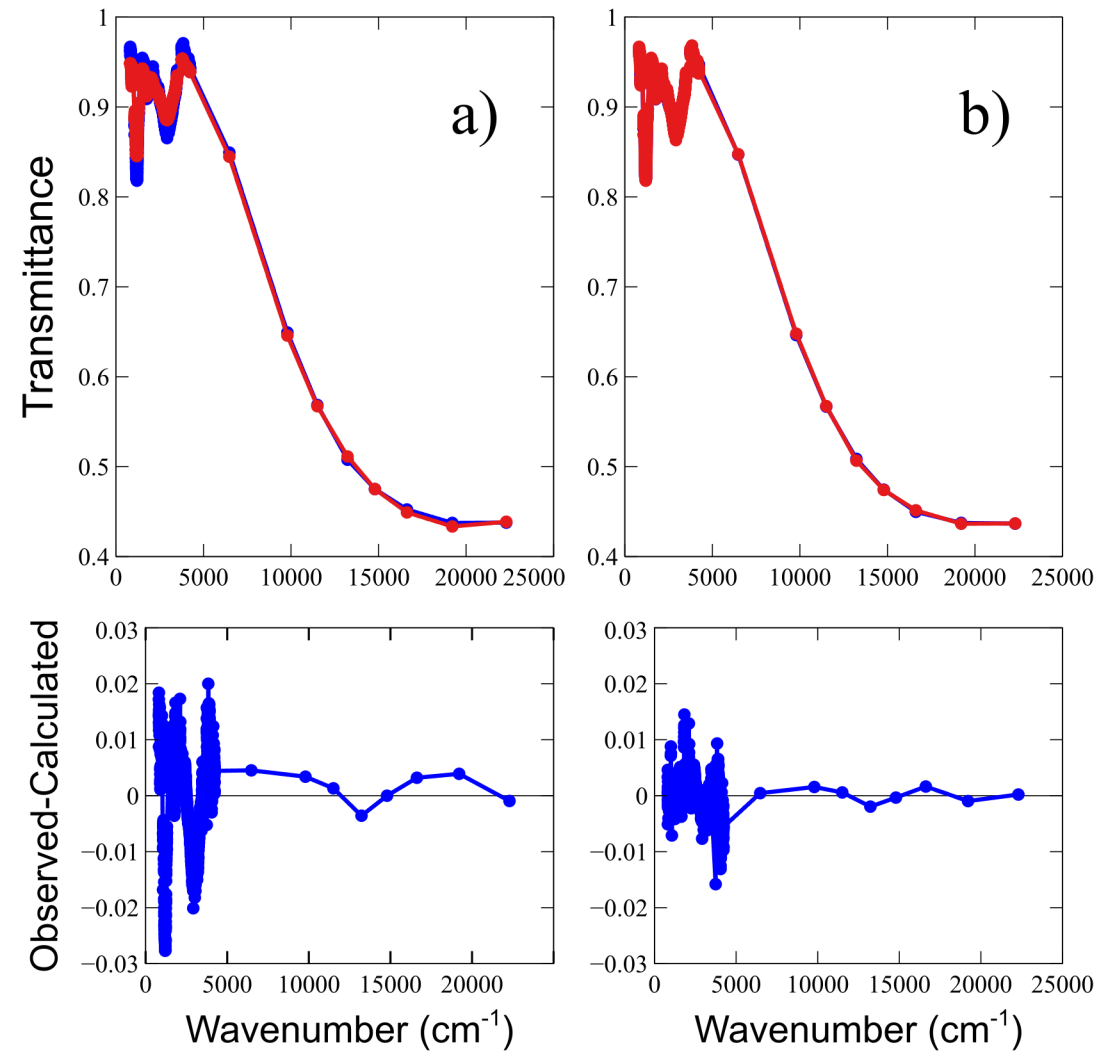


**Figure 4:** Combined ACE-FTS and SAGE III/ISS transmittance fitting results for the measurement at tangent height 23.6 km in ACE occultation ss100628. The coincident SAGE event is 2022041609. The top plots show the measurement in blue and the fitted result in red, while the bottom plot shows the residuals (observed – calculated). a) Assuming a monomodal distribution. b) Assuming a bimodal distribution.

# Background SSAs

- Again, bimodal distribution shows improvement of the spectral fit & IR region seems underestimated
- Dip around  $13228\text{ cm}^{-1}$  in SAGE data ( $\text{O}_2$  A-band?) might suggest the spectral feature of  $\text{O}_2$  is not completely removed from the dataset product for SAGE

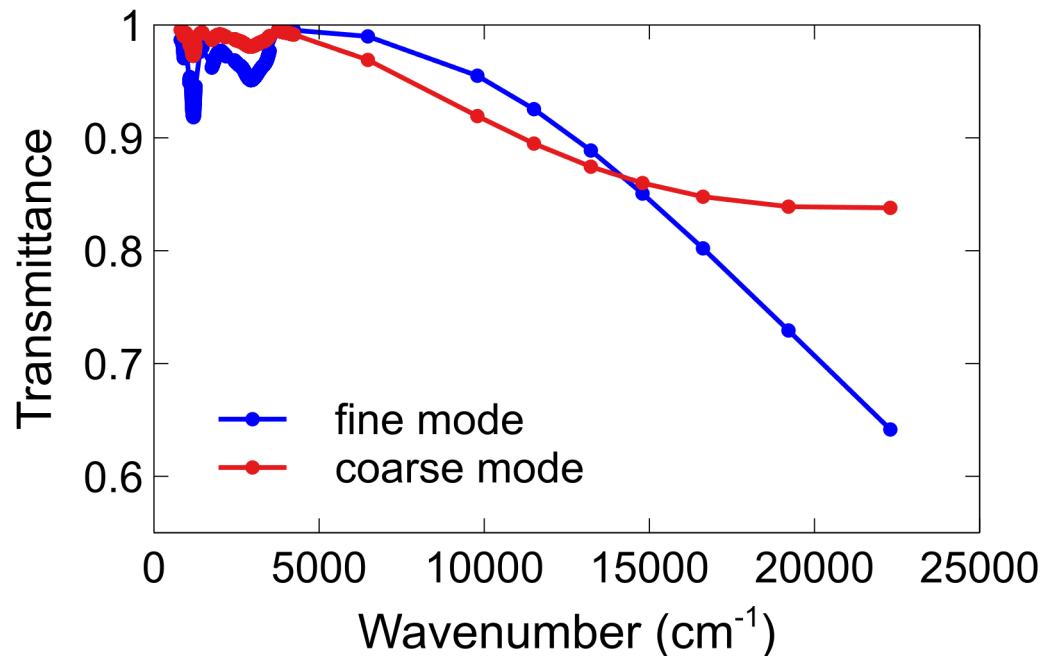


**Figure 7:** Contributions to the calculated spectrum for the bimodal fitting result in Figure 6 from the fine and coarse modes (in blue and red, respectively). The calculated spectrum is the product of the two curves.  $r_m(\text{fine}) = 0.053 \pm 0.002\ \mu\text{m}$ ,  $S(\text{fine}) = 1.65$  (fixed),  $r_m(\text{coarse}) = 0.27 \pm 0.01\ \mu\text{m}$ ,  $S(\text{coarse}) = 1.40$  (fixed), and  $N_o(\text{fine})/N_o(\text{coarse}) \approx 200$ . Reported uncertainties are random fitting errors and do not include systematic errors.

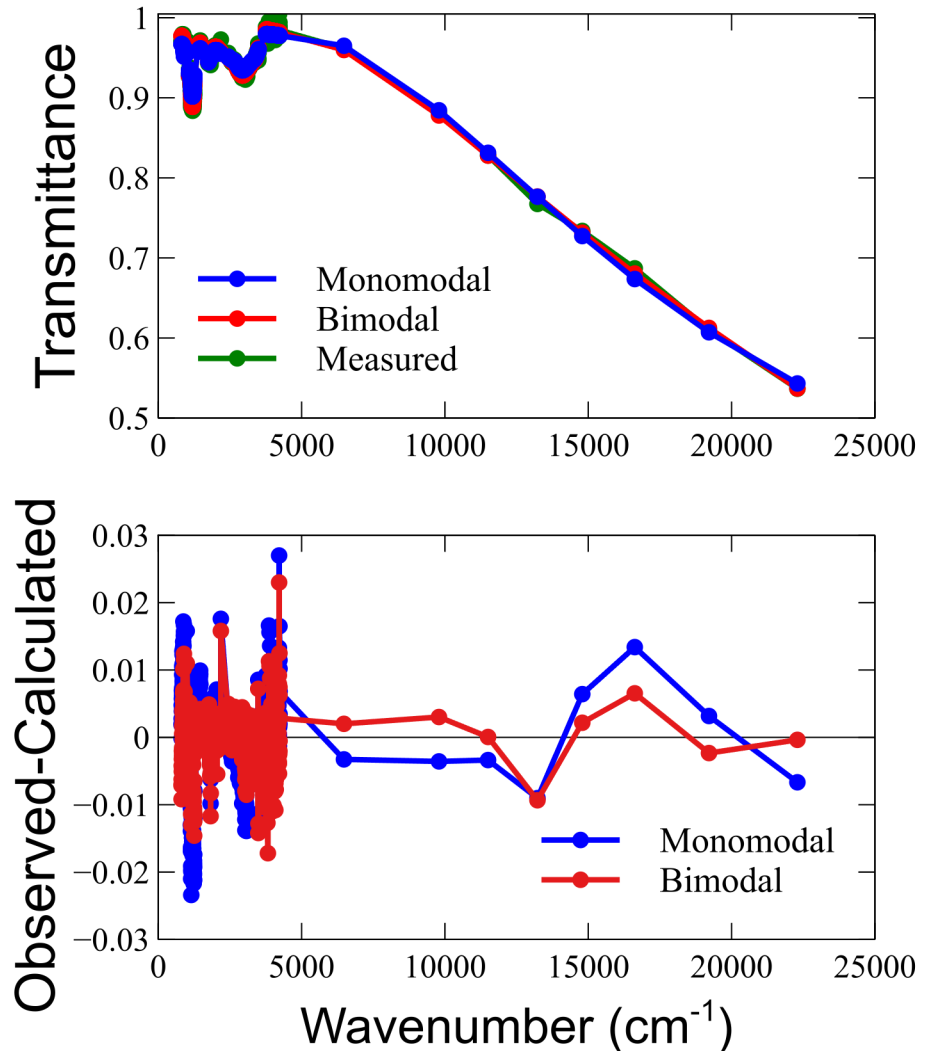


**Figure 6:** Combined ACE-FTS and SAGE III/ISS transmittance fitting results for the background measurement at tangent height 13.3 km in ACE occultation ss84200. The coincident SAGE event is 2019033036. The top plot shows the measurement in green, the bimodal fitted result in red, and the monomodal fitting result in blue. The bottom plot shows the fitting residuals (observed – calculated), with the bimodal results plotted in red and the monomodal results in blue.

# Comparison of results

$$r_{eff} = \frac{\int r^3 n(r) dr}{\int r^2 n(r) dr}$$

- Effective radii
- Tonga radii larger
- Raikoke and background similar
- With time, Raikoke values tend to approach background values (brown-youngest)

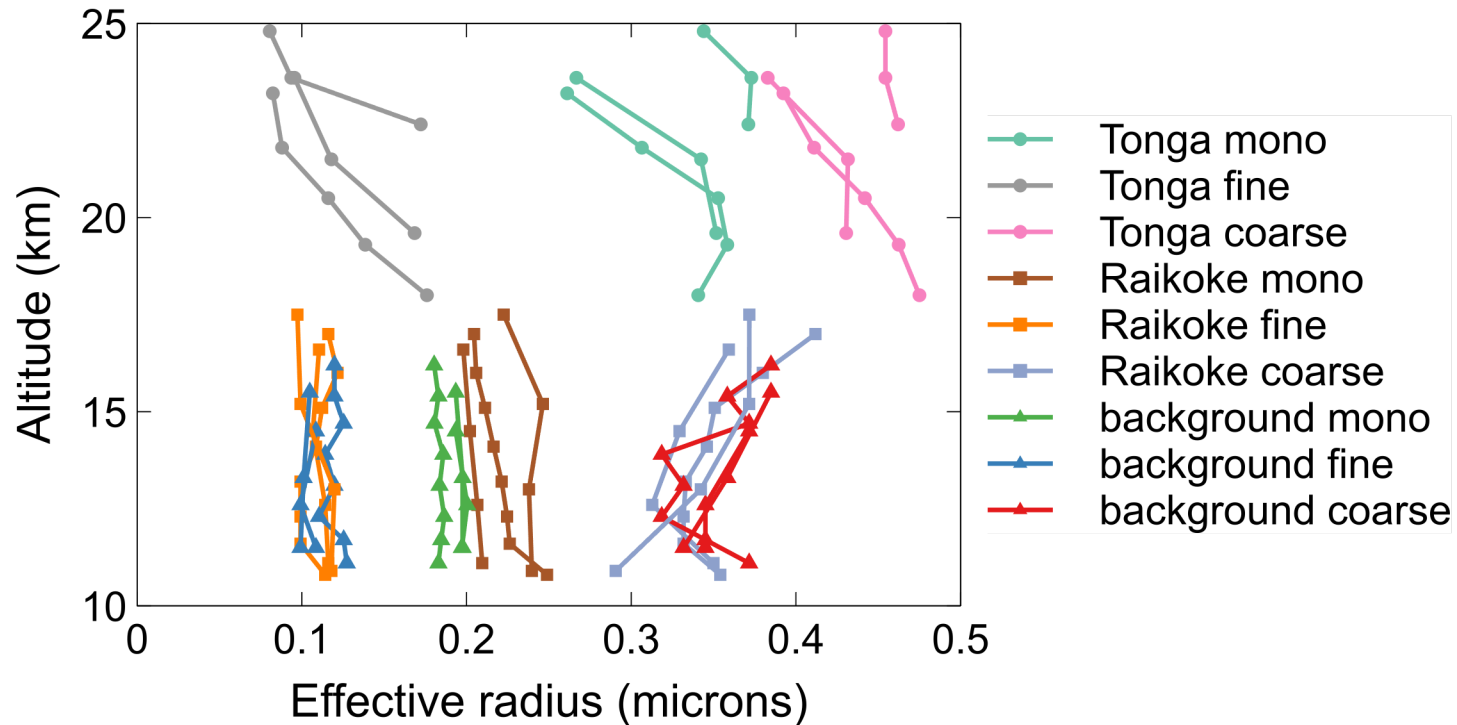


**Figure 8:** Effective radius profiles for the example occultations, including monomodal and bimodal (fine and coarse mode) lognormal distributions. Results are calculated from the size distribution information in Tables 2 through 4. Each curve is from a different occultation.



# Conclusions

- Our equation for the SSAs composition works best for  $T > 205$  K and can be used in various climate and chemical transportation models for volcanic eruptions
- The derived model is designed for volcanic plumes but would likely apply to background SSAs as well (versatile due to thermodynamic nature)
- Combined ACE / SAGE spectra are better reproduced by use of bimodal distribution
- By use of monomodal distribution derived from shortwave measurements one may likely underestimate the role of IR absorption and its role on surface heating of Earth
- Combination of both IR/VIS measurements with respect to bimodal distribution (particle size) yields the best and most precise results